agriculture

MDPI

Article

Staged Temperature- and Humidity-Controlled Combined Infrared Hot-Air Drying (TH-IRHAD) of Sea Buckthorn Reduces Drying Time, Energy Consumption, and Browning

Lichun Zhu [1], Xinyu Ji [1], Junzhe Gu [1], Xuetao Zhang [1], Mengqing Li [1], Qian Zhang [1,2,*], Xuhai Yang [1,2,3] and Zhihua Geng [1,*]

[1] College of Mechanical and Electrical Engineering, Shihezi University, 221 Beisi Road, Shihezi 832003, China; 20202009008@stu.shzu.edu.cn (L.Z.); 20211012426@stu.shzu.edu.cn (X.J.); 20221009235@stu.shzu.edu.cn (J.G.); 20232009039@stu.shzu.edu.cn (X.Z.); limengqing@stu.shzu.edu.cn (M.L.); yxh_513@shzu.edu.cn (X.Y.)
[2] Xinjiang Production and Construction Corps Key Laboratory of Modern Agricultural Machinery, 221 Beisi Road, Shihezi 832000, China
[3] Engineering Research Center for Production Mechanization of Oasis Special Economic Crop, Ministry of Education, Shihezi 832000, China
* Correspondence: zq_mac@shzu.edu.cn (Q.Z.); gzhjdxy@shzu.edu.cn (Z.G.); Tel.: +86-15299902258 (Q.Z.); +86-0993-2057550 (Z.G.)

Abstract: Sea buckthorn has garnered significant attention owing to its nutritional richness; however, it has a limited shelf life. In this study, the drying process of sea buckthorn was categorized into the first-, second-, and third-drying stages. Regression models were employed to examine the effects of the drying temperature, relative humidity of the medium, and prolonged high humidity retention on various parameters during the first- and second-drying stages. Comparative analysis revealed that the optimal drying conditions for the first-drying stage of sea buckthorn were a drying temperature of 80 °C, relative humidity of 28%, and high humidity retention time of 84 min. In the second-drying phase, the optimal conditions were a drying temperature of 78 °C, a relative humidity of 17%, and a high humidity retention time of 84 min. One-way optimization revealed that the optimal drying temperature for the third-drying stage was 70 °C. The implementation of temperature- and humidity-controlled infrared hot-air drying (TH-IRHAD) techniques considerably improved the outcomes. Specifically, the drying time, energy consumption, and degree of browning decreased by 34.43%, 36.29%, and 21.43%, respectively, whereas the brightness, rehydration ratio, total flavonoid content, and total phenol content increased by 8.94%, 16.99%, 20.57%, and 28.32%, respectively. Staged TH-IRHAD substantially reduced the drying duration, increased the efficiency, and enhanced the drying quality.

Keywords: sea buckthorn; temperature-humidity-controlled infrared hot-air drying (TH-IRHAD); process optimization; drying kinetics; drying quality

Citation: Zhu, L.; Ji, X.; Gu, J.; Zhang, X.; Li, M.; Zhang, Q.; Yang, X.; Geng, Z. Staged Temperature- and Humidity-Controlled Combined Infrared Hot-Air Drying (TH-IRHAD) of Sea Buckthorn Reduces Drying Time, Energy Consumption, and Browning. *Agriculture* **2024**, *14*, 743. https://doi.org/10.3390/agriculture14050743

Academic Editor: Zhi Huang

Received: 1 April 2024
Revised: 1 May 2024
Accepted: 5 May 2024
Published: 10 May 2024

1. Introduction

Sea buckthorn (*Hippophae rhamnoides* L.), a genus within the Hippophae family, is the primary species found in the Three North Protective Forests (TNPFs) in China [1,2]. It has also been cultivated in other countries, including the United States, Canada, Russia, Mongolia, Finland, Poland, and Germany [3]. Due to its resilience to light, cold, and heat, as well as its adaptability to sandy soils and arid climates, sea buckthorn is extensively utilized for soil and water conservation and desert greening. As of 2021, global sea buckthorn cultivation spanned 2.430 million hectares, with 2.410 of them located in China alone. These areas collectively yield an average of 650,000 tons of sea buckthorn annually, with a maximum global production of 800,000 tons [4].

The incidence of various chronic non-communicable diseases can be reduced by increasing daily fruit and vegetable consumption [5]. Sea buckthorn is an agricultural product

rich in nutrients such as vitamins, fatty acids, flavonoids, and carotenoids [6]. In recent years, public awareness of its anti-cancer, anti-aging, and anti-inflammatory properties, as well as its ability to treat and prevent gastrointestinal, cardiovascular, and cerebrovascular disorders, has gradually increased consumer recognition of sea buckthorn [7]. Nevertheless, the thin peel, juicy flesh, and extreme perishability make it challenging to store fresh sea buckthorn fruit at room temperature after harvest. Therefore, drying sea buckthorn fruit has been proposed as a viable solution to extend the shelf life and address issues related to shipping and storage.

The drying of sea buckthorn significantly influences the quality and production costs of the final dried product [8]. The drying process comprises two main stages: reduced-speed drying and constant-speed drying. Reduced-speed drying involves the diffusion of moisture from the inside to the outside of the material, a process influenced by the material's characteristics and primarily controlled by internal conditions. Constant-speed drying entails the transfer of energy from the surroundings to the material's surface to induce the evaporation of surface moisture [9]. During this stage, the drying rate is contingent upon the medium's temperature, humidity, and flow rate.

Numerous studies have investigated drying processes and technologies. According to the study of Ju et al. [10], applying 50% relative humidity in the early stage and 20% relative humidity in the later stage can shorten the drying time of carrot slices by 18.50%, and at the same time, delay the time of material crust formation. It is concluded that adjusting the relative humidity can transfer the internal water of the material to the surface in a timely fashion, so that the temperature of the material presents the trend of a step change. Curcio et al. [11] concluded that when the hot-air drying temperature is 45 °C and the wind speed is 1.5 m/s, the increase rate of the carrot surface temperature under 30% relative humidity is significantly higher than that under 10% relative humidity. Zhang et al. [12] studied yam tablets and found that the drying time of dehumidification and drying was 14.3% shorter than that of constant relative humidity. These investigation revealed that increasing the relative humidity of the medium is conducive to improving the product quality, but drying is a changing process; high-temperature drying is conducive to shortening the drying time, but the quality deteriorates seriously; the low-temperature drying quality is better, but the cycle is long and the energy consumption is large.

This study explores the impact of different temperatures, humidity levels, and high-humidity retention times on the drying characteristics and quality resulting from multi-stage variable-temperature drying. Our objective is to optimize the process parameters for drying sea buckthorn in terms of criteria such as the drying time, energy consumption, and third-drying quality indicators, including the color, luster, total phenol, flavonoids, vitamin C, rehydration ratio, and browning.

2. Materials and Methods

2.1. Test Materials and Devices

A TH-IRHAD test platform, manufactured by the Drying Laboratory of the School of Mechanical and Electrical Engineering at Shihezi University, was employed for the sea buckthorn drying test [13]. Fresh sea buckthorn fruit were picked from Emin County, 170 Regiment of the 9th Division of Xinjiang Production and Construction Corps. Sea buckthorn fruit of uniform size, consistent color and no scars and rots were hand-selected (varieties of big fruit late autumn red, average weight 0.52 ± 0.10 g, average initial moisture content of 81.91% ± 0.50%). The fruit were stored in the refrigerator at −20 °C. Subsequently, the dryer was activated, and the temperature and humidity settings were configured.

During the experiments, the dryer operated continuously for 30 min. After achieving stable operation, 100 g of sea buckthorn was placed at a loading density of 0.10 kg/m^2 onto stainless steel metal grid trays, which were, in turn, positioned inside the drying chamber. The drying process concluded when the moisture content of the wet base, Mt, fell below 10%. Upon cooling, the trays were sealed and packaged. Each drying experiment was repeated three times, and the results were averaged for analysis.

2.2. Test Method

The drying stage was divided into three phases: first-drying stage (dry-base moisture content: $Mt > 3$ g/g), second-drying stage (2 g/g $\leq Mt \leq 3$ g/g), and third-drying stages ($Mt < 2$ g/g). Three test types were employed to optimize each of these drying stages:

- Test 1: In the first-drying stage, the response surface was used to optimize the drying temperature, medium relative humidity and high humidity holding time. In the second- and third-drying stages, the drying temperature was 75 °C and the medium relative humidity was 10%.
- Test 2: The optimal drying process from test 1 was adopted in the first-drying stage; the response surface was used to optimize the drying temperature, medium relative humidity and high humidity holding time in the second-drying stage; and the drying temperature of 75 °C and medium relative humidity of 10% were adopted in the third-drying stage to dry to the end point.
- Test 3: In the first-drying stage, the optimal drying process from test 1 was adopted, and in second-drying stage, the optimal drying process from test 2 was adopted. Since the preliminary experiment had shown that when the relative humidity of the medium in the drying chamber exceeded 10% in the third-drying stage, the drying time and energy consumption would increase and the quality would decrease, only the single-factor test was used to determine the drying temperature in the third-drying stage.

2.2.1. Determining the Kinetics of Drying Sea Buckthorn

The drying moisture ratio (*MR*) and drying rate (*DR*) were estimated at various drying stages in terms of the drying time (*DT*) using the isochronous sampling and weighing method. The *MR*-*t* and *DR*-*DT* curves were plotted based on the changes in the sea buckthorn moisture content.

Equation (1) was utilized to determine the *MR* [14] of sea buckthorn at drying time t:

$$MR = \frac{M_t - M_e}{M_0 - M_e} \tag{1}$$

where M_0 is the initial dry-base moisture content, unit g/g; M_e is the dry-base moisture content when drying to equilibrium, unit g/g; and M_t is the moisture content of the dry base at any drying moment t, unit g/g.

Since the equilibrium dry basis moisture content, M_e, is much smaller than M_0 and M_t, Equation (1) can be simplified to Equation (2) [15]:

$$MR = \frac{M_t}{M_0} \tag{2}$$

The drying rate of sea buckthorn during the drying process can be calculated using Equation (3) [16]:

$$DR = \frac{M_{t_1} - M_{t_2}}{t_2 - t_1} \tag{3}$$

Several factors, including moisture diffusion, influence the drying of sea buckthorn. To investigate the interaction between these factors, the moisture migration rate during sea buckthorn drying was quantified using the effective moisture diffusivity (D_{eff}) [17]. A more precise estimation of the D_{eff} in sea buckthorn drying was achieved by employing Weibull's distribution function [18]. This choice was made because Fick's second law struggles to accurately describe the drying process unless uniform moisture distribution inside the sea buckthorn, constant temperature, and negligible material shrinkage are achieved during drying. Thus, *MR* can be expressed as Equation (4):

$$MR = \exp\left[-\left(\frac{\mathrm{t}}{\alpha}\right)^{\beta}\right] \tag{4}$$

where β is a dimensionless parameter related to the shape of the drying curve, and α is a constant scale parameter representing the rate of the drying process.

Equation (5) is employed to compute the shape parameter for the Weibull distribution function, facilitating the estimation of sea buckthorn deflection during drying [18]:

$$D_{eff} = \frac{D_{cal}}{R_g} = \frac{r^2}{\alpha R_g} \tag{5}$$

where R_g is a parameter related to the geometric size of the material, equal to 13.1 m^2/s for spherical sea buckthorn; r is the equivalent radius of sea buckthorn, set at 0.6 cm; and D_{cal} is the effective moisture diffusion coefficient estimated during sea buckthorn drying.

The dependence of the effective moisture diffusivity on the temperature is generally described by an Arrhenius-type relationship:

$$D_{eff} = D_0 exp\left[-\frac{E_a}{\mathrm{R}(T + 273.15)}\right] \tag{6}$$

where D_0 is the effective moisture diffusivity at a temperature tending to infinity (m^2/s); E_a is the active energy (kJ/mol); R is the universal gas constant, which has 8.314 J/mol·K as its value; and T is the drying temperature (°C).

The drying activation energy, E_a, for sea buckthorn was determined using Equation (7) [19], which was obtained by applying the natural logarithm on both sides of Equation (6):

$$\ln D_{eff} = \ln D_0 - \frac{E_a}{R}\frac{1}{(T + 273.15)} \tag{7}$$

The specific energy consumption (SEC) during the experiment (kW·h/kg), derived from Equation (8) [20], can be employed to determine the energy consumption of the sea buckthorn drying process:

$$SEC = \frac{1000W}{m_0\varphi_0 - m_i\varphi_i} \tag{8}$$

where W denotes the difference between the electric consumption before and after the experiment (kW·h); m_0 and m_i denote the initial and final mass (g) of the experimental material, respectively; and φ_0 and φ_i denote the initial and final wet-base moisture content (%) of the material for drying, respectively.

2.2.2. Determination of Physical and Chemical Properties of Sea Buckthorn after Drying

(1) Determination of color and browning degree

A colorimeter was utilized to measure the color of both fresh and dried sea buckthorn [21]. To assess the color, fresh sea buckthorn seeds were removed and the remaining part was transformed into a paste. For dried sea buckthorn, the seeds were removed too, and the remaining part was ground in an ice bath until reaching a powdered consistency. The color measurement was conducted on material passing through a No. 40 mesh. Following the measurement of the brightness (L^*), red–green (a^*), and yellow–blue (b^*) values, Equation (9) was employed to calculate the overall color difference (ΔE) in the material:

$$\Delta E = \sqrt{\left(L^* - L_0^*\right)^2 + \left(a^* - a_0^*\right)^2 + \left(b^* - b_0^*\right)^2} \tag{9}$$

where the L_0^*, a_0^*, b_0^* and L^*, a^*, b^* values denote the color characteristics of fresh and dried sea buckthorn, respectively.

To determine the browning degree (NEB), the approach reported by Chu et al. [22] was employed with some adjustments. A total of 2.0 g of sea buckthorn powder was combined with 20 mL of distilled water, homogenized, and then centrifuged at 10,000 rpm and 4 °C for 30 min. The absorbance value of the supernatant at 420 nm was used to quantify the

browning degree. To ensure the accuracy, absorbance values exceeding 1.0 were diluted in equal parts to bring them below 1.0, and the values were reported on a dry basis.

(2) Determination of rehydration ratio

The rehydration ratio was determined by the approach of Wang et al. [21]. A glass cup filled with deionized water was immersed in a water bath at 40 °C, maintaining a constant temperature. A specific amount of dried sea buckthorn was added to the water and allowed to steep for 12 h. The material's surface was then dried using absorbent paper, and the mass of the rehydrated sea buckthorn was measured using a balance. Equation (10) was employed to calculate the rehydration ratio, R_r (g/g):

$$R_r = \frac{m_2}{m_1} \tag{10}$$

where m_1 and m_2 are the masses (g) of the material before and after rehydration, respectively.

(3) Quantification of antioxidant content

To determine the vitamin C (Vc) level in sea buckthorn [19], after weighing 1.0 g of sea buckthorn powder in a mortar, 20 mL of a solution containing 20 g/L of oxalic acid was added. The mixture was then homogenized into a paste while in an ice bath and subsequently centrifuged at 8000 rpm for 10 min. The calculation utilized the 2,6-dichlorophenol indophenol reverse titration method to eliminate the impact of the sample solution's color. The Vc concentration in the samples was expressed on a dry basis (mg/100 g DW) and determined using Equation (11):

$$A = \frac{c \cdot V_1 \cdot V_2}{V_3 \cdot W} \times 100\% \tag{11}$$

where V_1 is the volume of Vc standard solution consumed by the titration of 5 mL of 2,6-dichloroindophenol sodium salt (mL), V_2 is the total volume of the sample solution, V_3 is the volume of the sample solution consumed by the titration of 5 mL of 2,6-dichloroindophenol sodium salt, and W is the dry weight of the sample (g).

The Vc retention rate (V), corresponding to the ratio of dried to fresh sea buckthorn Vc content, was used to compare the dried and fresh samples:

$$V = \frac{A_c}{A_x} \times 100\% \tag{12}$$

where A_c is the measured Vc content, and A_x is the Vc content of fresh sea buckthorn.

The total flavonoids in the samples were extracted using a 95% ethanol solution, and the extract was subjected to ultrasonic treatment at 80 °C and 200 W for 35 min [23]. After centrifuging the extract at 4 °C and 8000 rpm for 10 min, the supernatant was collected as the test solution. Using a UV spectrophotometer, 1.5 mL of the test solution was mixed with 1.5 mL of 5% $NaNO_2$, 0.15 mL of 10% $AlCl_3$, 1 mL of 4% NaOH, and 0.85 mL of distilled water. Equation (13) was employed to calculate the total flavonoid content (TFC) of the sample, which was reported in mg of rutin equivalent per g (mg RE/g DW):

$$TFC = \frac{x \cdot V \cdot n}{m} \tag{13}$$

where V is the extract volume (mL), n is the number of dilutions, m is the sample mass (g), and x is the experimentally observed total flavonoid concentration (mg/mL).

Sample extracts, obtained using the total flavonoid extraction method, were used to determine the total phenol content. Using a UV spectrophotometer, 0.4 mL of the test solution was mixed with 2 mL of 10% forintol and 3 mL of 10% Na_2CO_3, and allowed to react away from light for two hours. The sample's absorbance value at 765 nm was then

measured [24]. The total phenol content (*TPC*) was computed using Equation (14) and the results were presented as mg of gallic acid equivalent per g of sample (mg GAE/g DW):

$$TPC = \frac{x \cdot V \cdot n}{m} \tag{14}$$

where V is the extract volume (mL), n is the number of dilutions, m is the sample mass (g), and x is the experimentally measured total phenol concentration (mg/mL).

(4) All-encompassing assessment technique

With the aid of a comprehensive evaluation method, the multi-objective optimization problem was streamlined into a single-objective optimization. The objectives of the drying process optimization included reducing the drying time and energy consumption, and improving the final-drying quality characteristics, including the ascorbic acid retention, *TPC*, *TFC*, *Rr*, *NEB*, and *L**.

To eliminate data variability, the evaluation indicators must be normalized. Equations (15) and (16) [25] were, respectively, employed to normalize the negative (browning degree, drying time, and energy consumption) and positive (*V*, *TPC*, *TFC*, *Rr*, and *NEB*) indicators:

$$s_z = \frac{x_i - x_{min}}{x_{max} - x_{min}} \tag{15}$$

$$s_f = \frac{x_{max} - x_i}{x_{max} - x_{min}} \tag{16}$$

where s_z is the normalized value of a positive indicator, s_f is the normalized value of a negative indicator, x_i is the actual value, and x_{max} and x_{min} are the maximum and minimum values of the indicator, respectively.

The composite score F under each drying process was calculated according to Equation (17):

$$F = s_1k_1 + s_2k_2 + s_3k_3 + s_4k_4 + s_5k_5 + s_6k_6 + s_7k_7 + s_8k_8 \tag{17}$$

where s_1, s_2, s_3, s_4, s_5, s_6, s_7, and s_8 are the normalized values of Vc retention, *TPC*, *TFC*, *Rr*, *L**, NEB, *DT*, and *SEC*, respectively, and k_1, k_2, k_3, k_4, k_5, k_6, k_7 and k_8 are the corresponding weights.

The expert scoring method was employed to determine the weights of Vc retention, *TPC*, *TFC*, *Rr*, *L**, *NEB*, *DT*, and *SEC*. The assigned weights were, respectively, 0.15, 0.15, 0.10, 0.10, 0.10, 0.15, 0.15, and 0.15. This was performed to maximize the drying quality concerning ascorbic acid retention, *TPC*, *TFC*, *Rr*, and *L**, while minimizing the *NEB*, *DT*, and *SEC*.

2.2.3. Validation of the Drying Model

By integrating the sea buckthorn drying characteristics obtained from the experimental data into the theoretical, empirical, and semi-empirical models commonly employed to describe the thin-layer drying of agricultural materials, we determined the optimal parameters for each model using the SPSS software (version 18.0). The fit of each model to the experimental data was then evaluated utilizing the coefficient of determination (R^2), the root-mean-square error (*RMSE*), and the sum of squares of the deviations (reduced Chi-squared, χ^2) [26]:

$$R^2 = \frac{\sum_{i=1}^{N} \left(MR_i - MR_{pre,i}\right)\left(MR_i - MR_{\exp,i}\right)}{\sqrt{\left[\sum_{i=1}^{N} \left(MR_i - MR_{pre,i}\right)^2\right]\left[\sum_{i=1}^{N} \left(MR_i - MR_{\exp,i}\right)^2\right]}} \tag{18}$$

$$RMSE = \left[\frac{1}{N}\sum_{i=1}^{N}\left(MR_{pre,i} - MR_{\exp,i}\right)^2\right]^{1/2} \quad (19)$$

$$\chi^2 = \frac{\sum_{i=1}^{N}\left(MR_{pre,i} - MR_{\exp,i}\right)^2}{N - n} \quad (20)$$

where $MR_{exp,i}$ and $MR_{pre,i}$ are the measured and predicted moisture ratios, respectively; N is the number of experimental measurements; and n is the number of constants in the model equation. The model that exhibited the best fit to the data was selected to describe the drying process of sea buckthorn.

2.3. Division of the Drying Process

As mentioned earlier, to further optimize the drying process and identify the optimal drying temperature, medium relative humidity, and high humidity duration for the different drying phases, we divided the drying process into three stages: first-drying ($M_t > 3$ g/g), second-drying (2 g/g $\leq M_t \leq 3$ g/g), and third-drying ($M_t < 2$ g/g). From the preliminary experiment, it was observed that during the first-drying stage ($M_t > 3$ g/g), the moisture ratio rapidly declines and the drying rate undergoes significant fluctuations, initially increasing and then decreasing. The drying rate varies during the second-drying stage (2 g/g $\leq M_t \leq 3$ g/g) and exhibits a gradually decreasing trend in the third-drying period ($M_t < 2$ g/g).

2.4. Data Analysis Techniques

Graphs were generated using Origin 2021 and Excel 2020. For the analysis of variance (ANOVA), Duncan's test of significance analysis was employed, setting a significance threshold of $p < 0.05$. Design-Expert 8 was utilized to conduct the Box–Behnken central composite test for linear regression and optimization.

3. Results

3.1. First-Drying Stage Variables for TH-IRHAD of Sea Buckthorn

3.1.1. Response Surface Optimization for the Initial Drying Stage

The preliminary test results revealed that drying sea buckthorn at temperatures <60 °C took approximately 40 h, leading to undesirable color deterioration and considerable nutrient degradation. Conversely, drying temperatures >80 °C blackened the sea buckthorn pericarp and reduced the phenolic and flavonoid contents, in turn, negatively affecting the fruit characteristics and quality. Therefore, temperatures between 60 °C and 80 °C were used. The preliminary test results indicated that increasing the relative humidity to >10% improved the quality and reduced drying time. By contrast, increasing the relative humidity to >40% was detrimental to the subsequent drying steps and ultimately increased the drying time. The preliminary test results guided the selection of three test factors: drying temperature (A), medium relative humidity (B), and high medium relative humidity duration (C). The specific settings and coding for each of the test factors are listed in Supplementary Table S1. For the response surface optimization design experiment, the response values were as follows: *DT*, Y1; *SEC*, Y2; *L**, Y3; *Rr*, Y4; *NEB*, Y5; *TFC*, Y6; *TPC*, Y7; and Vc retention, Y8. After completing the tests in the first-drying stage for each group, the drying temperature was 75 °C and the relative humidity of the medium was 10% in the second- and third-drying stages to dry sea buckthorn to the safe moisture content.

3.1.2. Quality Evaluation during the First-Drying Stage

The results from the sea buckthorn quality analysis of the first-drying stage are shown in Table 1. The drying temperature (A) was identified as the primary factor influencing the drying time and energy consumption. Specifically, maintaining a high temperature during the first-drying phase lowered the energy consumption and shortened the drying time. The relative humidity during the first stage of drying was identified as the primary factor

influencing sea buckthorn browning after drying (B). After the estimation of the first-drying temperature, an increase in the relative humidity of the medium is expected to gradually reduce the extent of the sea buckthorn browning. Furthermore, a high humidity retention time (C) during the first-drying phase was identified as the primary factor influencing sea buckthorn brightness. An increase in the high humidity retention initially led to an increase in brightness, followed by a decrease, after the achievement of the first-drying temperature. The results show that the sea buckthorn brightness was enhanced after drying when certain conditions are met: an optimal first-drying temperature, a prolonged humidity holding time, and a high relative humidity in the medium. The first-drying temperature (A) was identified as the primary factor influencing the sea buckthorn rehydration ratio after drying. The Vc retention ratio of sea buckthorn after drying was primarily contingent on the relative humidity (B) of the first-drying medium. When a high-to-medium relative humidity was maintained for a specific period, the Vc retention rate increased gradually with the medium relative humidity. This phenomenon can be attributed to the reduction in the oxygen concentration in the drying medium and limited contact between Vc and oxygen in the high humidity environment, which slows down the Vc oxidation reaction. The nucleophilic substitution interaction between the water molecules and hydroxyl groups in Vc in a high humidity environment inhibits the breakdown and oxidation of Vc [19]. The primary factor influencing the total flavonoid and phenol contents of sea buckthorn after drying was the first high humidity holding duration (C).

Table 1. Analysis of the drying quality of sea buckthorn in the first-drying stage.

	AB (Treatment Time/min-Medium Humidity/%)	**AC (Drying Temperature/°C-Treatment Time/min)**	**BC (Medium Humidity/%-Treatment Time/min)**
Drying time/ min	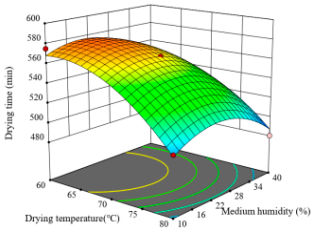	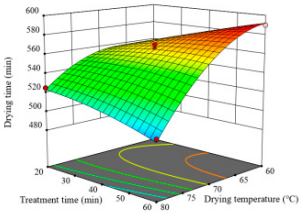	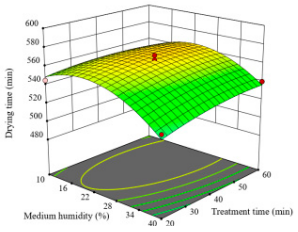
SEC/ $kW{\cdot}h{\cdot}kg^{-1}$	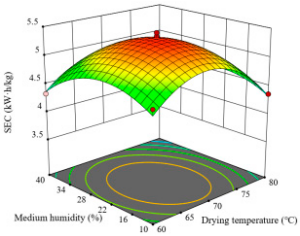	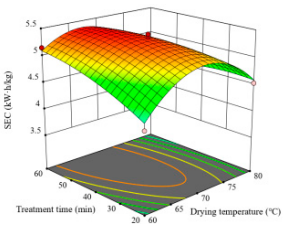	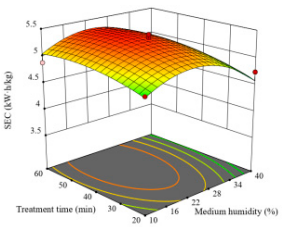
NEB/ $Abs{\cdot}g^{-1}$ d.m.	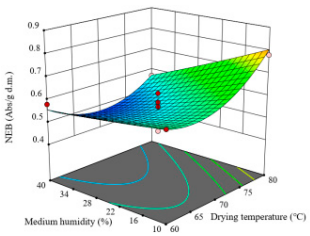	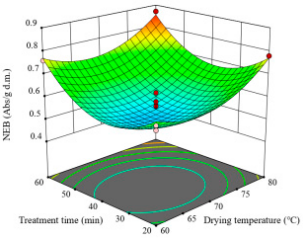	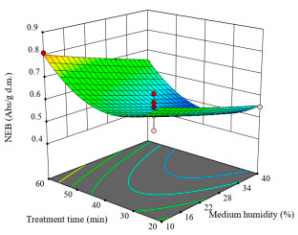
*L**	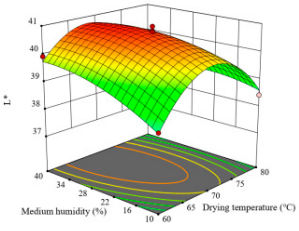	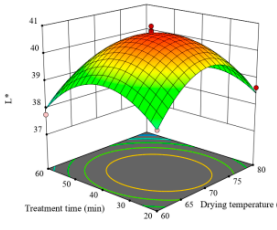	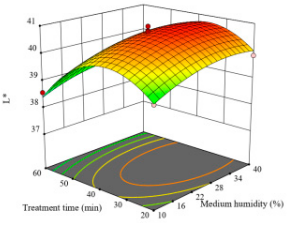

Table 1. *Cont.*

	AB (Treatment Time/min-Medium Humidity/%)	AC (Drying Temperature/°C-Treatment Time/min)	BC (Medium Humidity/%-Treatment Time/min)
Rr/ $g \cdot g^{-1}$	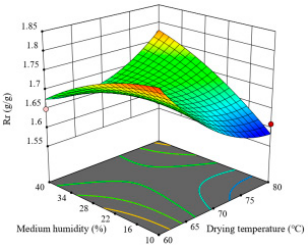	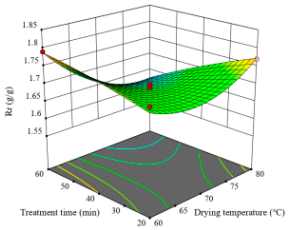	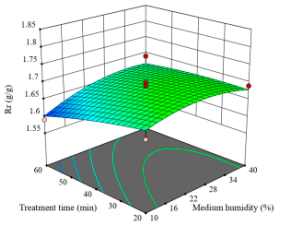
Vc/ %	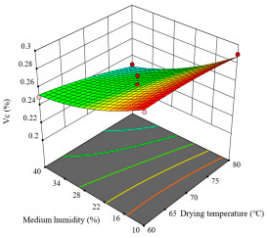	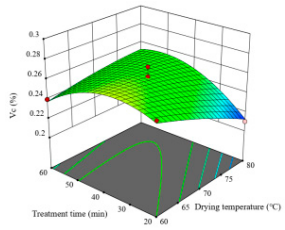	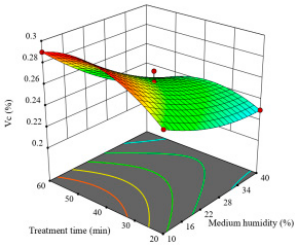
TFC/ mg RE·g^{-1} DW	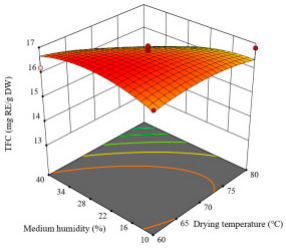	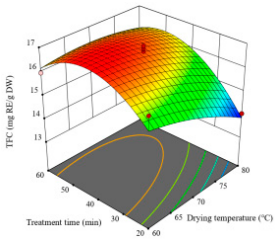	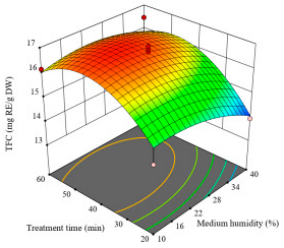
TPC/ mg GAE·g^{-1} DW	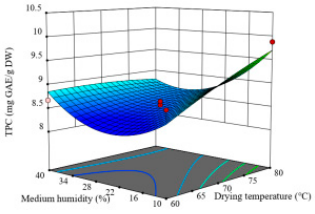	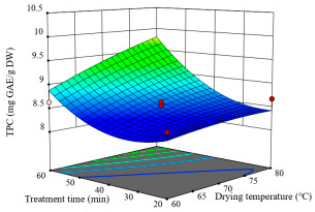	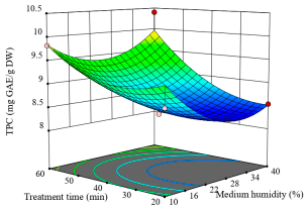

3.1.3. Optimized Parameters for First-Drying Stage

The characteristics of high-quality dried sea buckthorn include high brightness, Vc retention rate, rehydration ratio, and total phenol and flavonoid contents. The drying process must be rapid and energy efficient, while also inducing a low level of browning. To establish an ideal criterion, the first 20 sets of results for each parameter combination were analyzed during sea buckthorn's first-drying stage using TH-IRHAD (Supplementary Table S2).

The optimal parameter combinations identified were as follows: first-drying temperature of 80 °C, medium relative humidity of 28.41%, and high humidity retention time of 59.85 min. Considering the actual production process for sea buckthorn, the optimization conditions were adjusted as follows: first-drying temperature of 80 °C, medium relative humidity of 28%, and high humidity retention time of 60 min. The validation results are presented in Supplementary Table S3. The results show model-optimized parameters for eight indices: drying time, energy consumption, browning degree, rehydration ratio, brightness, Vc retention, and total phenol and flavonoid contents. The optimization of sea buckthorn TH-IRHAD during the first-drying stage proved reliable. The relative error between the actual and predicted model values was <5%, and the experimental values closely matched the predicted values.

3.2. Second-Drying Stage Variables for TH-IRHAD of Sea Buckthorn

3.2.1. Response Surface Optimization for Second-Drying Stage

The initial stage of sea buckthorn drying was completed using the first-drying response surface optimized conditions: a drying temperature of 80 °C, relative humidity of 28%, and high humidity retention time of 60 min. A response surface optimization design experiment conducted for the middle stage of the sea buckthorn drying process guided the selection of test factors. The factors included the drying temperature (A), medium relative humidity (B), and medium relative humidity duration (C). The settings and coding for each factor are listed in Supplementary Table S4. For the response surface optimization design experiment, the response values were as follows: *DT*, Y1; *SEC*, Y2; *L**, Y3; *Rr*, Y4; *NEB*, Y5; *TFC*, Y6; *TPC*, Y7; and Vc retention, Y8. The sea buckthorn was dried to a safe moisture content during the late-drying stage using a drying temperature of 75 °C. A medium relative humidity of 10% was applied after the completion of each test in the middle of drying for each group.

3.2.2. Quality Evaluation during Second-Drying Stage

The results of the sea buckthorn middle-stage quality analysis are presented in Table 2. The drying temperature (A) was identified as the primary factor influencing the drying duration during the middle stage. Sea buckthorn can be dried faster by increasing the drying temperature and medium relative humidity during the middle stage and maintaining them for a while. The medium relative humidity (B) was identified as the primary factor influencing the amount of energy used during the middle-stage drying process. A high-temperature and low-humidity environment was identified as the most beneficial condition for reducing the drying energy consumption. In comparison, the medium-term drying temperature (A) was the key factor affecting the degree of sea buckthorn browning after drying. The primary factor influencing the sea buckthorn brightness after drying was the medium-stage relative humidity (B). Sea buckthorn's brightness increases with an increase in the storage duration and at lower relative humidity levels when the medium-term drying temperature is known. The medium-term drying temperature (A) was identified as the primary factor influencing the third-drying stage Vc retention rate, rehydration ratio, and overall phenolic content of the sea buckthorn. After drying, the medium-term mean relative humidity (B) was identified as the primary factor influencing the total flavonoid concentration in sea buckthorn.

Table 2. Analysis of the drying quality of sea buckthorn in the second-drying stage.

	AB (Treatment Time/min-Medium Humidity/%)	**AC (Drying Temperature/°C-Treatment Time/min)**	**BC (Medium Humidity/%-Treatment Time/min)**
Drying time/min	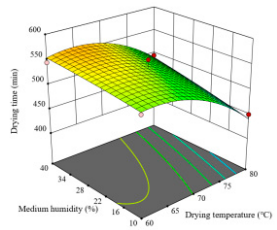	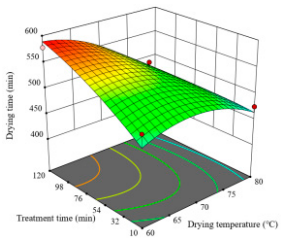	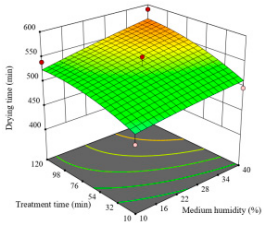
SEC/kW·h·kg^{-1}	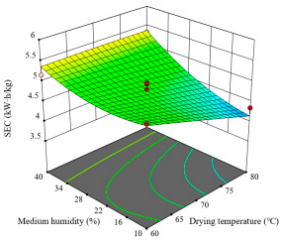	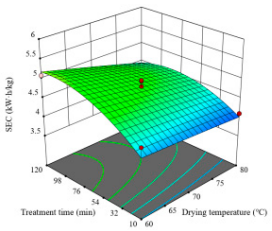	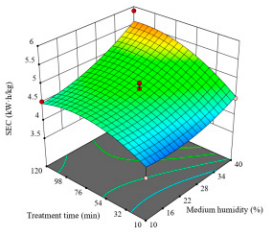

Table 2. *Cont.*

	AB (Treatment Time/min-Medium Humidity/%)	AC (Drying Temperature/°C-Treatment Time/min)	BC (Medium Humidity/%-Treatment Time/min)
NEB/Abs·g^{-1} d.m.	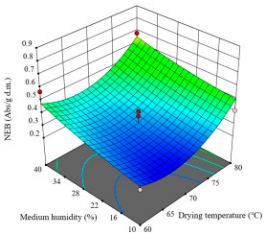	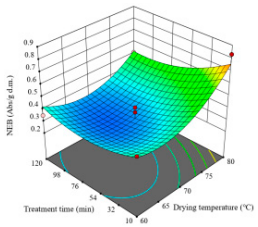	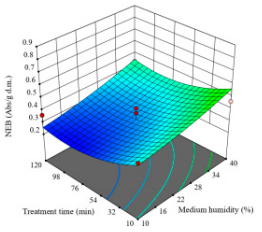
*L**	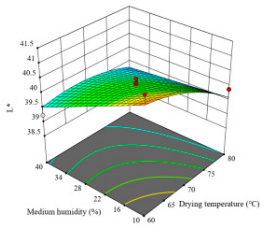	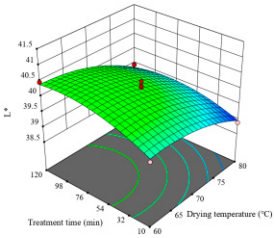	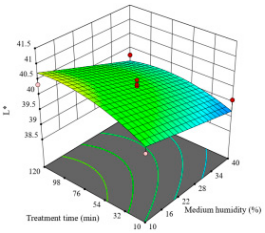
Rr/g·g^{-1}	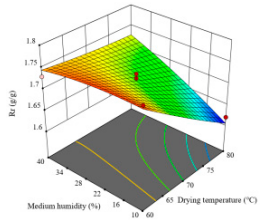	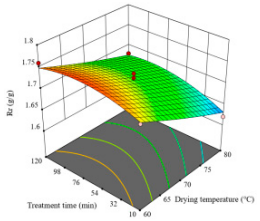	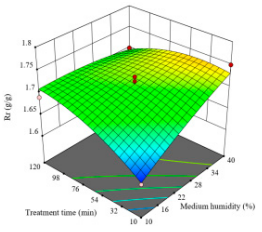
Vc/%	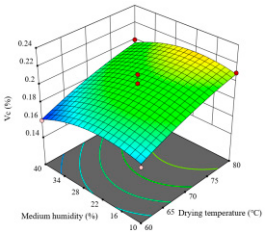	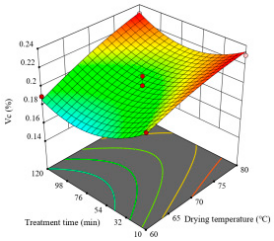	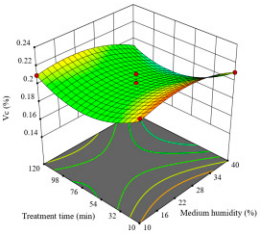
TFC/mg RE·g^{-1} DW	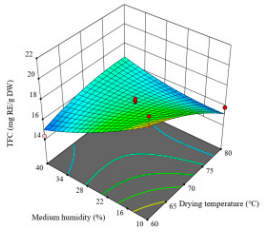	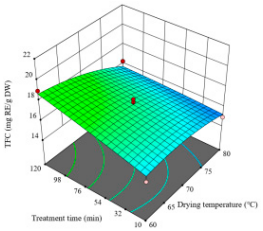	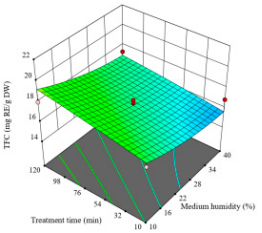
TPC/mg GAE·g^{-1} DW	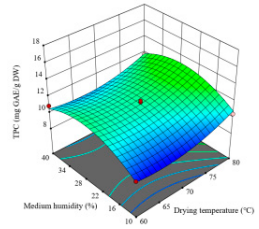	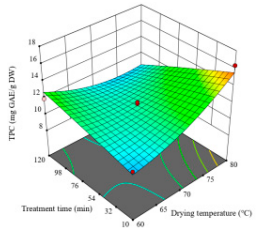	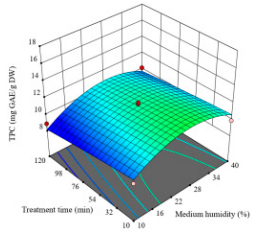

3.2.3. Optimized Parameters for Second-Drying Stage

The ideal parameter combination for the medium-term TH-IRHAD of sea buckthorn was obtained by analyzing the data and setting the response variables. The outcomes for the first 20 groups are presented in Supplementary Table S5. A medium-term drying temperature of 78.32 °C, medium relative humidity of 16.60%, and high humidity retention

duration of 84.31 min were identified as the ideal parameter combination. To account for the realities of production, the parameters were modified as follows: a medium-term drying temperature of 78 °C, medium relative humidity of 17%, and high humidity retention duration of 84 min. The validation results and actual values are shown in Supplementary Table S6. The results show that the experimental values were close to the predicted values, with the relative errors between the actual and predicted values of the model being less than 5%. Therefore, these results indicate that the parameter optimization was reasonable, the statistical analysis was valid, and the optimization results of the medium-term drying process were useful.

3.3. Third-Drying Stage Variables for TH-IRHAD of Sea Buckthorn

3.3.1. Response Surface Optimization for the Third-Drying Stage

The ideal temperature for the third-drying stage was determined using a one-way test based on the optimal drying process identified for the first-test and second-drying stages. The first-test showed that increasing the relative humidity of the medium in the third-drying stage had no significant effect on improving the drying quality but prolonged the drying time. To investigate the third-drying stage process for sea buckthorn, nine different drying models were selected to fit the change curves of the drying moisture ratio with the drying times at different temperatures. In addition, six different drying qualities, namely, color, total phenols, flavonoids, Vc content, rehydration ratio, and browning, were evaluated. The experimental setup and associated parameter values are listed in Supplementary Table S7.

3.3.2. Quality Evaluation during the Third-Drying Stage

(1) Impact of drying temperature on drying kinetics

For the third-drying stage of sea buckthorn ($MR \leq 0.4$ g/g), the relative humidity was adjusted to 10% and various temperatures were tested. The drying characteristic curves for sea buckthorn are shown in Figure 1a,b, and the variation curves for the moisture ratio with the drying time are shown in Figure 1a. During the third-drying stage ($MR \leq 0.4$ g/g), the drying time was reduced from 1026 to 363 min by increasing the drying temperature from 60 °C to 80 °C. Specifically, the drying times at 80 °C were 663, 390, 214, and 90 min shorter than those at 60 °C, 65 °C, 70 °C, and 75 °C, respectively. The drying temperature greatly influenced the duration of the third-drying stage ($MR \leq 0.4$ g/g). Higher drying temperatures resulted in a faster moisture decrease and a shorter drying time, in line with the findings of Deng et al. [19].

The variation curves for the sea buckthorn drying rate with the dry-base water content at various drying temperatures (60 °C, 65 °C, 70 °C, 75 °C, and 80 °C) are shown in Figure 1b. The drying rate changed temporarily when the sea buckthorn IRHAD reached the later stage ($MR \leq 0.4$ g/g and dry-basis water content $Mt < 1.9$ g/g), as shown in Figure 1b. In this context, a dry-base water content >2.8 g/g indicates the first-drying stage, while a range of 1.9–2.8 g/g indicates the second-drying stage, and 2.8 g/g indicates the junction point between the first- and second-drying stages. Increasing the drying temperature improved the drying rate; however, the quality of the drying was extensively degraded at higher temperatures. The drying rate increased with an increase in the temperature, and the drying temperature had a significant effect on the drying rate during the late drying period ($MR \leq 0.4$ g/g). The results indicate that the drying temperature affected the water diffusion inside sea buckthorn. An inflection point arose during the first-drying and middle stages of the drying process. This phenomenon could be attributed to the fact that the evaporation of free water was altered during the drying process, which is comparatively easier to remove than bound water.

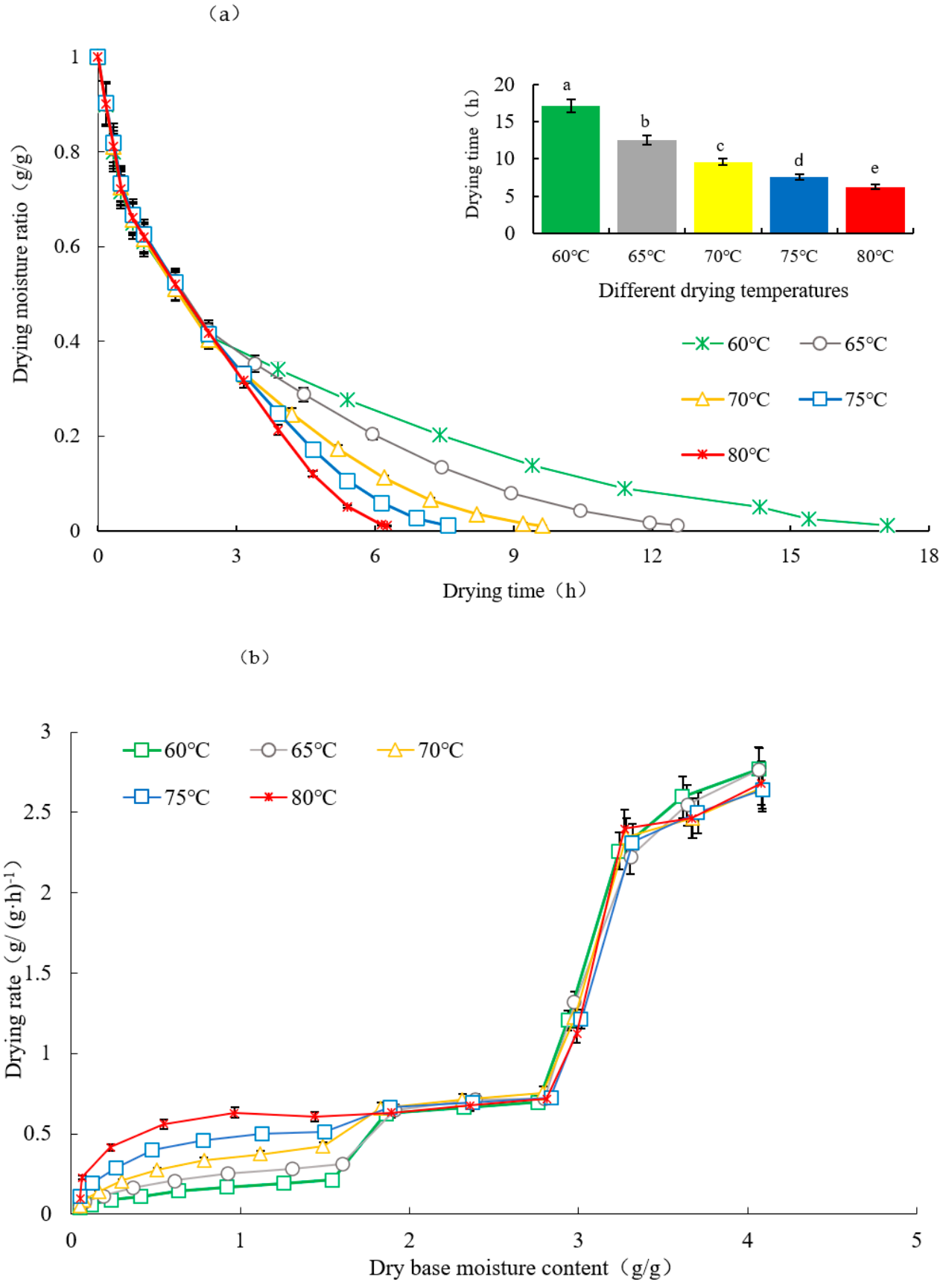

Figure 1. *Cont.*

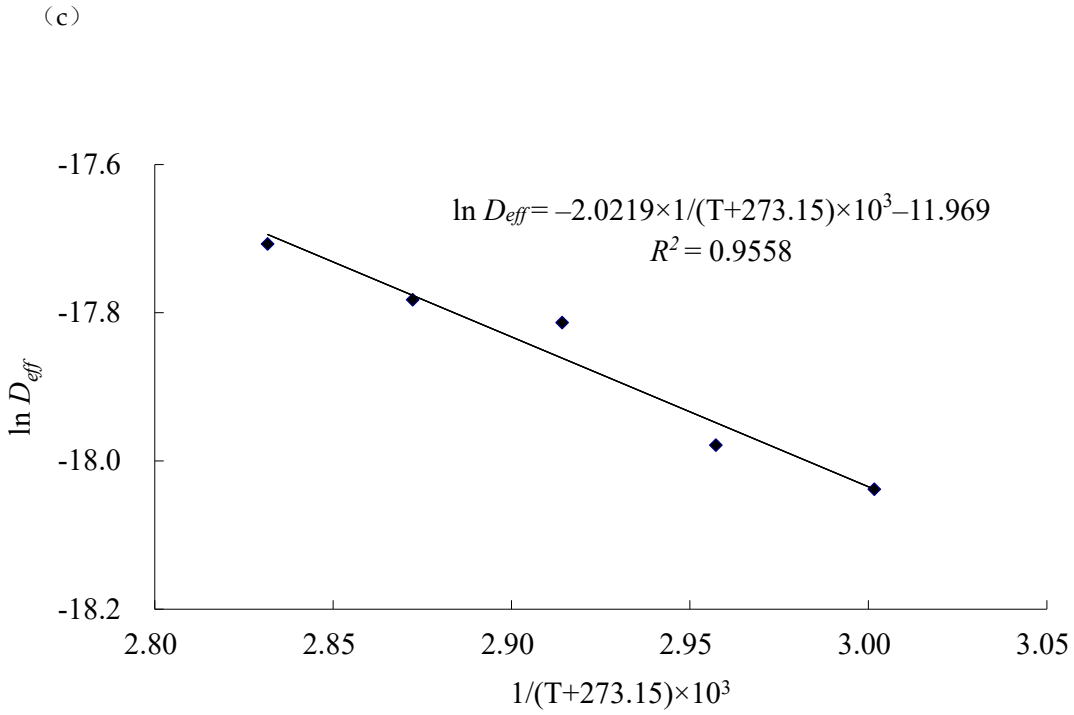

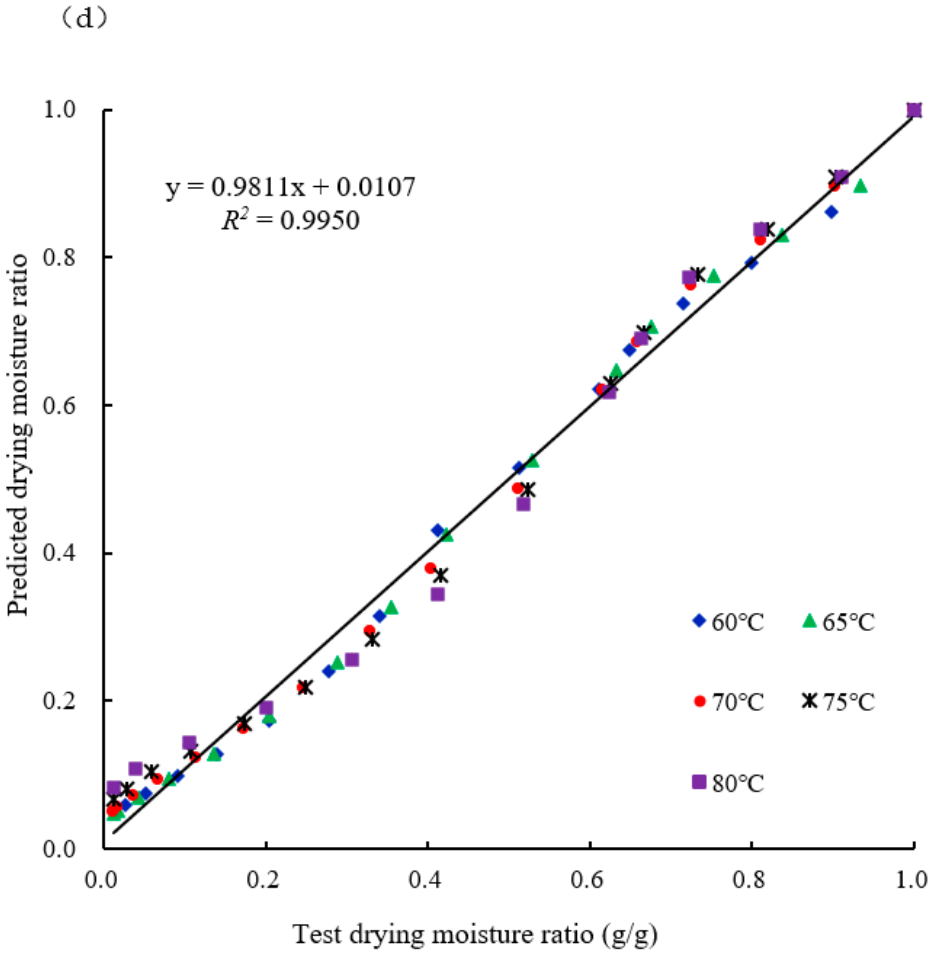

Figure 1. *Cont.*

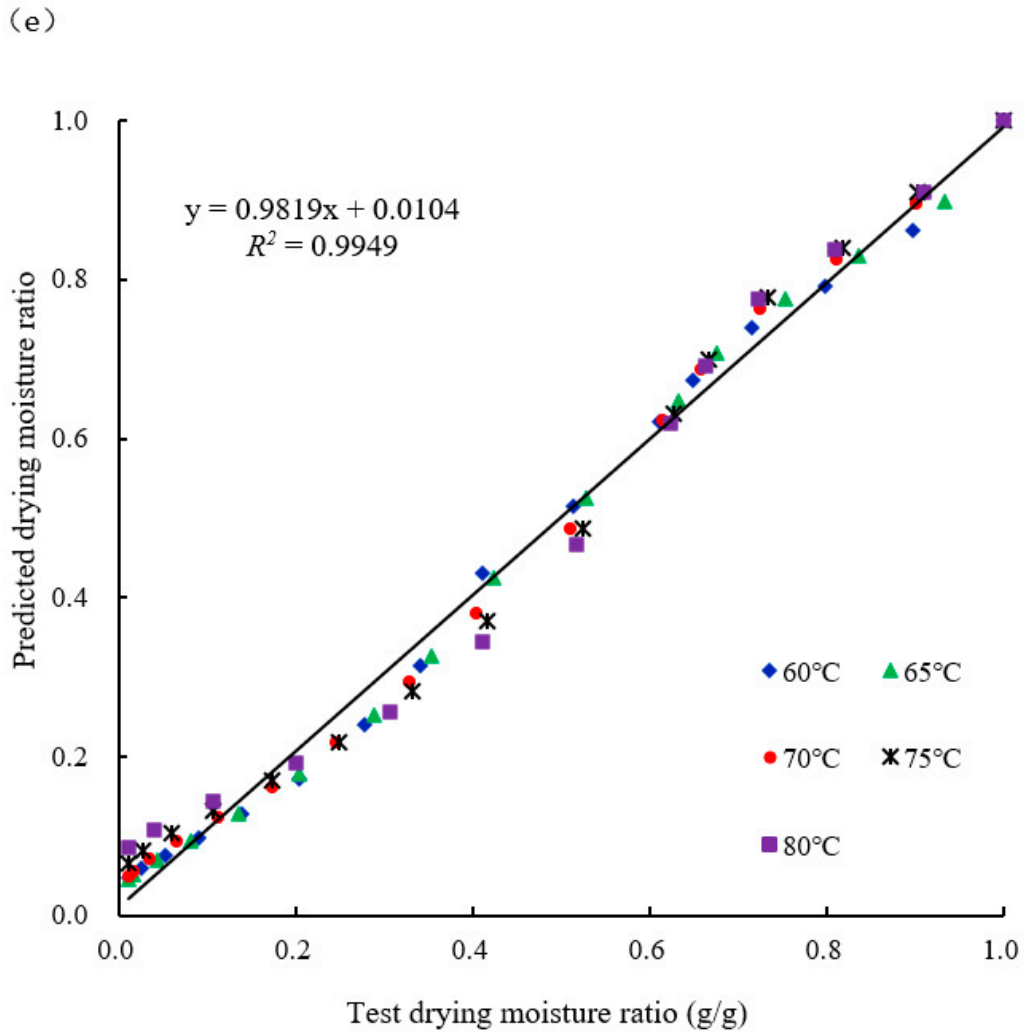

Figure 1. (**a**) Curves of the dry moisture ratio of sea buckthorn with the drying time at different drying temperatures. (**b**) Curves of the drying rate ratio of sea buckthorn with the dry base moisture content at different drying temperatures. (**c**) Fitting curve of the effective water diffusion coefficient and drying temperature in the drying process of sea buckthorn. (**d**) Experimental values of the moisture ratio and Page model predicted values under different drying conditions. (**e**) Experimental values of the moisture ratio and Weibull model predicted values under different drying conditions. Note: Different letters indicate significant differences in the samples ($p < 0.05$).

(2) Impact of the drying temperature on the moisture activation energy and an effective diffusion coefficient

The Weibull function was used to determine the effective diffusion of moisture in sea buckthorn, and the findings are presented in Supplementary Table S8. The effective diffusion coefficients for sea buckthorn water were 1.47×10^{-8} m^2/s, 1.56×10^{-8} m^2/s, 1.84×10^{-8} m^2/s, 1.89×10^{-8} m^2/s, and 2.04×10^{-8} m^2/s when the drying temperatures were 60 °C, 65 °C, 70 °C, 75 °C, and 80 °C, respectively. The effective diffusion coefficient of water in sea buckthorn increased with an increase in the temperature, reaching 10^{-8} m^2/s. The effective diffusion coefficient for water at 80 °C was 1.39-times greater than that at 60 °C, indicating that a high temperature may generate more energy to facilitate water diffusion from inside to outside. Similar conclusions have been reported by several researchers [25,27,28].

The activation energy during the drying process can reflect the difficulty of sea buckthorn drying and can be used to estimate the drying energy consumption [19]. Based on the relationship between the effective diffusion coefficient of moisture and the drying

temperatures of sea buckthorn when using IRHAD, the activation energy of sea buckthorn drying was determined to be 16.81 kJ/mol. Most agricultural goods have drying activation energies ranging between 12.7 and 111.0 kJ/mol, and these energies vary depending on the drying technique. Comparatively, sea buckthorn has a higher drying activation energy than apricots [27], goji berries [29], and blueberries [25]. However, it has a lower drying activation energy than grapes [28] and saint fruits [30]. Such variations can be attributed to variations in the chemical compositions and organizational structures of the materials. Moreover, the diverse chemical makeup and arrangement of the materials may result in the subsequent variations in the activation energies associated with their respective drying processes.

(3) Mathematical models for various drying temperatures

The Weibull model fitted better than the other eight models tested, with a coefficient of determination (R^2) and a sum of squared deviations χ^2 of 0.99436 at a drying temperature of 60 °C (Table 3). The Weibull model showed a best fit and a goodness of fit (0.99489) at 65 °C, while the Verma model showed the best fit at 70 °C and 80 °C, with corresponding goodness-of-fit values of 0.99499 and 0.98361, respectively. The Weibull and Page models were the most accurate when predicting the sea buckthorn kinetic curve during the TH-IRHAD process.

Table 3. Regression results from the fitting of the model to the moisture ratio change.

Model Name and Equation	Drying Temperature	Model Constants	*R*2	*RMSE*	χ2
Lewis $MR = \exp(-kt)$	60 °C	$k = 0.00569$	0.93363	0.10734	0.00716
	65 °C	$k = 0.00572$	0.97420	0.04489	0.00299
	70 °C	$k = 0.00661$	0.98099	0.03252	0.00217
	75 °C	$k = 0.00681$	0.98282	0.02709	0.00193
	80 °C	$k = 0.00740$	0.97742	0.03022	0.00252
Page $MR = \exp(-kt^n)$	60 °C	$k = 0.03304$; $n = 0.65161$	0.99436	0.00912	0.00065
	65 °C	$k = 0.01839$; $n = 0.77232$	0.99489	0.00889	0.00064
	70 °C	$k = 0.01701$; $n = 0.81343$	0.99415	0.01000	0.00071
	75 °C	$k = 0.01277$; $n = 0.87616$	0.98823	0.01856	0.00143
	80 °C	$k = 0.01170$; $n = 0.90738$	0.98041	0.02623	0.00238
Modified Page $MR = \exp[(-kt)^n]$	60 °C	$k = 0.07355$; $n = 0.07746$	0.93363	0.10734	0.00767
	65 °C	$k = 0.07563$; $n = 0.07563$	0.97420	0.04489	0.00321
	70 °C	$k = 0.08131$; $n = 0.08131$	0.98099	0.03252	0.00232
	75 °C	$k = 0.08252$; $n = 0.08252$	0.98282	0.02709	0.00208
	80 °C	$k = 0.08603$; $n = 0.08603$	0.97742	0.03022	0.00275
Henderson and Pabis $MR = a\exp(-kt)$	60 °C	$k = 0.00419$; $a = 0.87054$	0.96652	0.05414	0.00387
	65 °C	$k = 0.00498$; $a = 0.92320$	0.98551	0.02521	0.00180
	70 °C	$k = 0.00590$; $a = 0.92814$	0.99070	0.01591	0.00114
	75 °C	$k = 0.00631$; $a = 0.94613$	0.98880	0.01766	0.00136
	80 °C	$k = 0.00696$; $a = 0.95721$	0.98160	0.02463	0.00224
Wang and Singh $MR = 1 + at + bt^2$	60 °C	$a = -0.00288$; $b = 1.99289 \times 10^{-6}$	0.79338	0.33413	0.02387
	65 °C	$a = -0.00360$; $b = 3.19296 \times 10^{-6}$	0.90666	0.16241	0.01160
	70 °C	$a = -0.00442$; $b = 4.90606 \times 10^{-6}$	0.93401	0.11293	0.00807
	75 °C	$a = -0.00491$; $b = 6.28902 \times 10^{-6}$	0.95859	0.06530	0.00502
	80 °C	$a = -0.00549$; $b = 7.93237 \times 10^{-6}$	0.96113	0.05203	0.00473
Approximation of diffusion $MR = a\exp(-kt) + (1 - a)\exp(-kbt)$	60 °C	$k = 0.00571$; $a = -3.55588 \times 10^{7}$; $b = 1$	0.93363	0.10734	0.00826
	65 °C	$k = 0.00572$; $a = 1$; $b = 1$	0.97420	0.04489	0.00345
	70 °C	$k = 0.00661$; $a = 1.00023$; $b = 1.00203$	0.98099	0.03252	0.00250
	75 °C	$k = 0.04744$; $a = 3.12557 \times 10^{14}$; $b = 1$	0.51441	0.76565	0.06380
	80 °C	$k = 0.00740$; $a = 1$; $b = 1$	0.97742	0.03022	0.00302
Verma $MR = a\exp(-kt) + (1 - a)\exp(-bt)$	60 °C	$k = 0.00378$; $a = 0.82315$; $b = 7.47134$	0.98079	0.03106	0.00239
	65 °C	$k = 0.00472$; $a = 0.89331$; $b = 8.00641$	0.99024	0.01698	0.00131
	70 °C	$k = 0.00562$; $a = 0.89833$; $b = 7.47132$	0.99499	0.00858	0.00066
	75 °C	$k = 0.00610$; $a = 0.92338$; $b = 7.47130$	0.99142	0.01353	0.00113
	80 °C	$k = 0.00676$; $a = 0.93733$; $b = 7.64572$	0.98361	0.02194	0.00219

Table 3. *Cont.*

Model Name and Equation	Drying Temperature	Model Constants	*R2*	*RMSE*	$\chi 2$
Two-term exponential $MR = a\exp(-kt) + (1-a)\exp(-kat)$	60 °C	$k = 0.02442$; $a = 0.17796$	0.96986	0.04874	0.00348
	65 °C	$k = 0.00281$; $a = 0.99814$	0.75204	0.43146	0.03082
	70 °C	$k = 0.00658$; $a = 0.99762$	0.98099	0.03254	0.00232
	75 °C	$k = 0.06519$; $a = 0.09261$	0.99167	0.01314	0.00101
	80 °C	$k = 0.00740$; $a = 1.00027$	0.97742	0.03022	0.00275
Weibull $MR = \exp(-(t/\alpha)^{\beta})$	60 °C	$\alpha = 187.43148$; $\beta = 0.65209$	0.99436	0.00912	0.00065
	65 °C	$\alpha = 176.57656$; $\beta = 0.77358$	0.99489	0.00889	0.00063
	70 °C	$\alpha = 149.67507$; $\beta = 0.815360$	0.99416	0.01000	0.00071
	75 °C	$\alpha = 145.14707$; $\beta = 0.87854$	0.98823	0.01856	0.00143
	80 °C	$\alpha = 134.61968$; $\beta = 0.91004$	0.98041	0.02622	0.00238

Notes: where *MR* is the moisture ratio, unit g/g; t is the drying time, unit min; and where both *n*, *k*, *a*, *b* are constants in the model equation.

The Page model has high prediction accuracy and can be used to predict changes in the moisture ratio during sea buckthorn TH-IRHAD at different drying temperatures. This was demonstrated by validating the predicted and experimental values of the Weibull and Page models (Figure 1d,e).

(4) Effects of drying temperature on energy consumption

The power consumption of sea buckthorn IRHAD is reflected in the energy consumption. A comparison of the drying energy consumption in the late-drying stage under various temperatures and a constant medium relative humidity of 10% is shown in Figure 2b. The results suggest that, at lower temperatures, more energy is used for each dehydration unit. For example, when dried at 80 °C, the amounts of energy used for each unit of dehydration were reduced by 2.87 kW·h/kg, 1.68 kW·h/kg, 0.99 kW·h/kg, and 0.47 kW·h/kg compared with those when drying at 60 °C, 65 °C, 70 °C, and 75 °C, respectively. This phenomenon could be attributed to the long drying period and prolonged operation of the dehumidification fan, electric heating film, and other factors. As the drying process is lengthy, the moisture-removal fan must be run for a long period, and the electric heating film and other electrical components use electricity, creating a positive association between the drying duration and the energy consumption of the unit during dehydration.

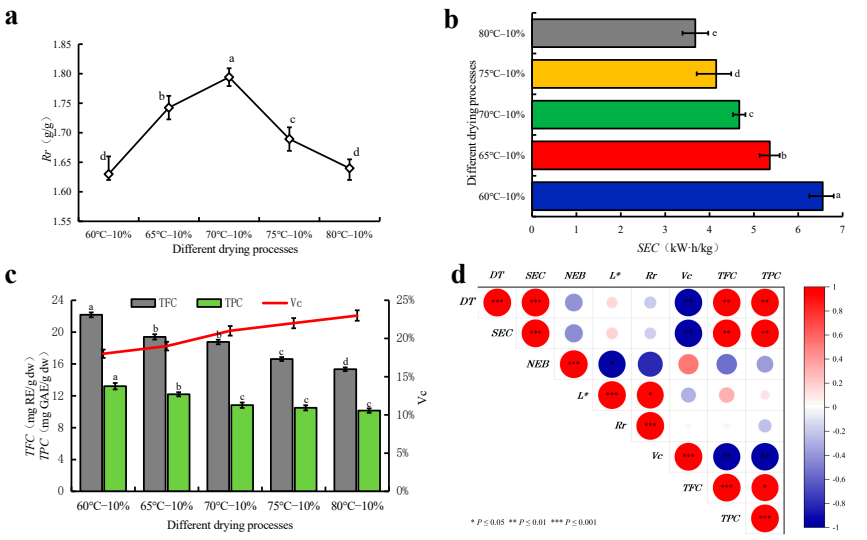

Figure 2. (**a**) Rehydration ratio curves of sea buckthorn at different drying temperatures. (**b**) Specific energy consumption (*SEC*) of sea buckthorn at different drying temperatures. (**c**) Content of antioxidant active substances in sea buckthorn at different drying temperatures. (**d**) Correlation matrixes between the determination parameters. Note: Different letters indicate significant differences in the samples ($p < 0.05$).

(5) Effect of drying temperature on color and browning

A significant difference was observed in the color of the fresh sea buckthorn and that of the fresh sea buckthorn after the various drying temperatures ($\Delta E > 22$). A difference in color was also observed visually between the groups; however, the difference was relatively low, which could be attributed to the data being collected after the sea buckthorn fruit were dried to extract the seeds. While the data differences were minor, they were nonetheless significant. There was a positive correlation between the measured color difference and the color observed by the naked eye. Changes in the brightness (L^*) and yellow–green value (b^*) were primarily responsible for the color changes. Among the various tested temperatures, the sea buckthorn ΔE was the lowest after drying at 70 °C, indicating that the dried fruit color was bright yellow and the change in color was significantly lower than that at the other temperatures ($p < 0.05$). This finding suggests that an optimal temperature is key for maintaining the color and luster of sea buckthorn [29].

Two critical factors when evaluating the quality of food products are color and luster, which significantly influence consumer preferences and product values [19]. Table 4 presents the color attributes (brightness (L^*), red–green (a^*), blue–yellow (b^*), and color difference (ΔE) values) of sea buckthorn samples that were subjected to infrared combined hot-air drying at a constant medium relative humidity of 10% across different drying temperatures. The color and luster of sea buckthorn improved with the increasing drying temperature, although a notable distinction was observed between the final-drying temperature and the L^* values of the dried fruit. When dried at 70 °C, the dried fruit exhibited the highest brightness, closely resembling fresh fruit. Temperatures of 80 °C and 78 °C were employed in the early and middle stages of the experiment, respectively. Consequently, employing a low temperature in the final stage prolonged the drying period and heightened the oxidative browning during the drying process. By contrast, maintaining a high drying temperature of 80 °C during the last stage caused the pasteurization of sugars in the sea buckthorn and the deterioration of the plant's color.

Table 4. Color parameters and browning degree of sea buckthorn at different drying temperatures.

Parameter	Different Drying Processes				
	60 °C-10%	**65 °C-10%**	**70 °C-10%**	**75 °C-10%**	**80 °C-10%**
L^*	40.51 ± 0.04^{d}	41.37 ± 0.10^{b}	41.92 ± 0.04^{a}	40.69 ± 0.03^{c}	40.09 ± 0.02^{e}
a^*	22.77 ± 0.04^{d}	22.89 ± 0.02^{c}	$23.31 \pm 0.07^{a,b}$	23.37 ± 0.07^{a}	23.25 ± 0.01^{b}
b^*	39.84 ± 0.09^{c}	40.89 ± 0.19^{b}	41.65 ± 0.10^{a}	39.94 ± 0.05^{c}	39.24 ± 0.03^{d}
ΔE	24.76 ± 0.07^{b}	23.50 ± 0.17^{d}	22.50 ± 0.06^{e}	24.32 ± 0.02^{c}	25.21 ± 0.03^{a}
NEB/(Abs/g DW)	0.40 ± 0.02^{b}	0.35 ± 0.01^{c}	0.33 ± 0.01^{c}	0.41 ± 0.02^{b}	0.48 ± 0.02^{a}

Note: Different letters indicate significant differences in the samples ($p < 0.05$).

Analysis of the a^* values revealed that sea buckthorn exhibited a reddish hue, given that the a^* values exceeded 22. However, with an increase in the temperature, the red–green values initially increased and then decreased, aligning with the changes in brightness. The observed pattern could be attributed to changes in the carotenoids and other pigments present in the plant. The use of appropriate drying temperatures was effective in preventing the loss of carotenoids, consistent with the findings of Jiang et al. [31] regarding Panax Pseudoginseng root drying. Sea buckthorn, characterized by b^* values exceeding 39, exhibited a vibrant yellow color, which is likely attributable to its high concentration of flavonoids. A decline in the flavonoid compound content may be associated with the extended drying period, resulting in flavonoid loss. The a^*, L^*, and b^* values exhibited a similar trend, indicating the pronounced influence of the late-drying temperature on the color profile.

Table 4 details the variations in the browning degree of sea buckthorn for different drying temperatures. The lowest degree of browning was observed after drying at 70 °C, followed by those measured after drying at 65 °C, 60 °C, 75 °C, and 80 °C. This trend is

consistent with the changes in the color difference, ΔE, suggesting that higher temperatures may induce enzymatic browning and oxidative reactions, consequently increasing the degree of browning. Additionally, the data revealed a negative correlation between the browning degree and L^*, consistent with the findings of Deng et al. [19].

(6) Impact of the drying temperature on the rehydration ratio

An essential metric for assessing dried products is the rehydration ratio, which can be used to describe the material destruction during the drying process [32]. A higher rehydration ratio is indicative of superior product quality because it reduces the degree of structural degradation caused by drying [33]. The effects of different drying temperatures on the rehydration ratios of sea buckthorn in the third-drying stage are shown in Figure 2a. Varying the drying temperature significantly impacted the rehydration properties, and the rehydration ratio tended to increase during the third-drying stage prior to declining. This could be because the material experienced crusting and the internal organizational structure of the sea buckthorn collapsed with the long low-temperature drying period in the third-drying stage. High-temperature drying during the third-drying stage, however, resulted in structural alterations to the sugar molecules, which, in turn, affected the rehydration [18].

(7) Effect of drying temperature on antioxidant substances

Vc, a nutrient vital to human health and abundant in sea buckthorn [20], is typically selected as an evaluation index during thermal processing owing to its thermal instability. Other nutrients are retained in addition to Vc [19]. The retention of Vc in sea buckthorn at different drying temperatures is shown in Figure 2c. After drying, at least 70% of the Vc was lost, which may be because Vc has poor thermal stability and is easily affected by the temperature; the drying time may also impact the Vc retention. The results also showed that the Vc retention in sea buckthorn increased gradually with an increase in the drying temperature, which may be related to the Vc loss caused by the duration of the drying time. Longer drying times prompted an increase in the Vc degradation at 80 °C, which increased the Vc retention in sea buckthorn, while Liu et al. [25] found that temperatures >75 °C increased the Vc degradation in blueberries. By contrast, ascorbic acid was well preserved in sea buckthorn at a drying temperature of 80 °C. This preservation can be attributed to the temperature being controlled by the TH-IRHAD device, which likely utilized the carbon fiber infrared heating plate and heating tube rather than relying solely on the properties of the material itself, which contrasts with hot-air drying that involves the rapid warming of the material while maintaining the environment at a constant temperature. The sea buckthorn was only at 70 °C when dried at 80 °C in this experiment. This lower temperature may effectively preserve the Vc content.

The total flavonoid concentration in sea buckthorn, when dried at various temperatures, is shown in Figure 2c. The results revealed that the total flavonoid content of sea buckthorn was inversely proportional to the drying temperature. Sea buckthorn had the highest flavonoid content after drying at 60 °C, which could be attributed to the lower drying temperature at the later stage, which allowed heat-sensitive flavonoids to be maintained to a greater extent than other components [34]. After drying, the phenolic contents demonstrated a notable decline with an increase in the drying temperature, similar to that of the flavonoids.

Correlation analysis (Figure 2d) revealed that the drying time and energy consumption were significantly and positively correlated ($p < 0.01$), indicating that shorter drying times lowered the drying energy consumption, and subsequently, lowered the energy consumption and total flavonoid and phenol contents ($p < 0.01$). This is because short drying times require high temperatures, and high temperatures inevitably degrade the total phenol and flavonoid contents—which are heat-sensitive—into other substances [27]. However, the drying time was significantly negatively correlated with the Vc retention rate; shorter drying times led to higher Vc retention rates, presumably because prolonged drying prevented Vc from degrading [19]. In addition, a highly significant negative correlation ($p < 0.05$) was found between browning and brightness. The Vc retention was significantly

negatively correlated ($p < 0.01$) with the total flavonoid and phenol contents; higher Vc retention corresponded to lower total flavonoid and phenol contents. The total flavonoid and phenol contents exhibited a significant positive correlation ($p < 0.05$); additionally, the brightness and rehydration ratio exhibited a significant positive correlation ($p < 0.05$). The trends were consistent; thus, the drying characteristics and quality of sea buckthorn in the late-drying stage can be assessed based on the following factors: total flavonoid content, total phenol content, browning, brightness, rehydration ratio, Vc retention, and drying time or energy consumption.

3.3.3. Optimized Parameters for the Third-Drying Stage

The comprehensive scoring technique yielded the highest results when applied to a drying temperature of 70 °C (Supplementary Table S9). Consequently, 70 °C was selected as the drying temperature for sea buckthorn in the late stages of TH-IRHAD.

3.4. Sea Buckthorn Quality When Dried at a Constant Temperature with Regulated Humidity

Consistent temperature and humidity levels were achieved using the TH-IRHAD system, which employed specific parameters for each drying stage. These parameters included a first-drying temperature of 80 °C, medium relative humidity of 28%, and high humidity retention time of 60 min; a second-drying temperature of 78 °C, medium relative humidity of 17%, and high humidity retention time of 84 min; and a third-drying stage drying temperature of 70 °C and medium relative humidity of 10%. The three drying methods used were infrared combined with hot-air drying, drying temperatures of 75 °C, medium relative humidity of 10%, and constant temperature and humidity. The quality analysis presented in Supplementary Table S10 shows that the three-stage TH-IRHAD reduced the drying time, energy consumption, browning, brightness, rehydration ratio, and Vc retention rate by 34.43%, 36.29%, 21.43%, 8.94%, 16.99%, and 25.00%, respectively. Additionally, the total number of drying methods were reduced. The drying process was performed by setting the parameters at 70 °C and 10% constant relative humidity. The three-stage TH-IRHAD reduced the drying time, energy consumption, degree of browning, and brightness by 0.52%, 17.20%, 26.92%, and 6.67%, respectively. The total flavonoid content increased by 20.57%, whereas the total phenol content increased by 28.32%. The rehydration ratio increased by 5.92%, and the Vc retention rate was reduced by 36.29%. Increases of 42.88% and 53.40% in the total flavonoid and phenol contents, respectively, were observed, along with a decrease of 33.50% in the Vc retention rate, an increase of 26.92% in the degree of browning, and a 6.67% increase in the brightness.

4. Conclusions

Multi-objective drying process parameters were investigated using sea buckthorn as the test material. The objective was to shorten the drying cycle and enhance the drying efficiency and quality, laying a foundation for the intelligent drying of sea buckthorn. The TH-IRHAD process was segmented into the first-, second-, and third-drying stages. For the first-drying stage, the ideal parameters for sea buckthorn were determined to be a drying temperature of 80 °C, medium relative humidity of 28%, and high humidity retention time of 60 min. For the second-drying stage, the optimal conditions were a drying temperature of 78 °C, relative humidity of 17%, and high humidity retention time of 84 min. The effects of the third-drying stage on the characteristics and quality of sea buckthorn were assessed using a one-way test, with evaluation by experts. The weights for each drying attribute (i.e., time and energy consumption) and quality factors (i.e., color, total phenol and flavonoid contents, Vc, rehydration ratio, and browning) were assigned based on expert scoring. A correlation matrix comparing the drying quality and energy consumption was established, which provided new insights and strategies for the sustainable development of the industry. Compared with constant TH-IRHAD, the staged temperature- and humidity-controlled approach significantly reduced the drying time, energy consumption, and browning, and it increased the brightness, rehydration ratio, and total flavonoid and phenol contents.

The implementation of TH-IRHAD considerably shortened the sea buckthorn drying time, increased the efficiency, and ensured that the dried product was of high quality.

Supplementary Materials: The following supporting information can be downloaded at: https://www.mdpi.com/article/10.3390/agriculture14050743/s1, Table S1: Factors and levels of response surface test in first-drying stages; Table S2: Optimal solution set in first-drying stages; Table S3: The results in first-drying stages optimum test were verified; Table S4: Factors and levels of response surface test in second-drying stages; Table S5: Optimal solution set in second-drying stages; Table S6: The results in second-drying stages optimum test were verified; Table S7: Experimental design and related parameters in third-drying stages; Table S8: Deff in the drying process of sea buckthorn at different temperatures; Table S9: Normalized results and comprehensive scores of index parameters at different drying temperatures; Table S10: Quality analysis of sea buckthorn under different drying methods.

Author Contributions: L.Z.: Conceptualization, writing—review and editing, investigation, formal analysis. Z.G.: Writing—review and editing. J.G.: Formal analysis, conceptualization. X.Z.: Investigation, formal analysis. Q.Z.: Writing—review and editing, investigation. M.L.: Formal analysis, investigation. X.J.: Supervision, project administration. X.Y.: Project administration, funding acquisition. All authors have read and agreed to the published version of the manuscript.

Funding: This work was supported by the Bingtuan Science and Technology Program (2023AB076, 2023CB016) and the Bingtuan Core Technology Program (NYHXGG, 2023AA503).

Institutional Review Board Statement: Not applicable.

Informed Consent Statement: Not applicable.

Data Availability Statement: The original contributions presented in this study are included in the article/supplementary material, further inquiries can be directed to the corresponding author.

Conflicts of Interest: The authors declare no conflicts of interest.

References

1. Song, Y.T.; Zhang, G.Y.; Chen, N.; Zhang, J.G.; He, C.Y. Metabolomic and transcriptomic analyses provide insights into the flavonoid biosynthesis in sea buckthorn (*Hippophae rhamnoides* L.). *LWT—Food Sci. Technol.* **2023**, *187*, 115276. [CrossRef]
2. Chang, X.M.; Sun, L.B.; Yu, X.X.; Liu, Z.Q.; Jia, G.D.; Wang, Y.S.; Zhu, X.H. Windbreak efficiency in controlling wind erosion and particulate matter concentrations from farmlands. *Agric. Ecosyst. Environ.* **2021**, *308*, 107269. [CrossRef]
3. Yu, L.Y.; Diao, S.F.; Zhang, G.Y.; Yu, J.G.; Zhang, T.; Luo, H.M.; Duan, A.G.; Wang, J.P.; He, C.Y.; Zhang, J.G. Genome sequence and population genomics provide insights into chromosomal evolution and phytochemical innovation of *Hippophae rhamnoides*. *Plant Biotechnol. J.* **2022**, *20*, 1257–1273. [CrossRef] [PubMed]
4. FAO. FaoStatDatabase. Available online: http://www.fao.org/faostat/en/#data/QC.2022 (accessed on 21 December 2022).
5. Garcia-llobodanin, L.; Billiris, A. Effect of the drying air conditions on the drying rate and milling quality of a long-grain rice variety. *Food Sci. Technol.* **2023**, *43*, e65722. [CrossRef]
6. Ma, Y.; Yao, J.X.; Zhou, L.; Zhao, M.J.; Wang, W.; Liu, J.K.; Marchioni, E. Comprehensive untargeted lipidomic analysis of sea buckthorn using UHPLC-HR-AM/MS/MS combined with principal component analysis. *Food Chem.* **2024**, *430*, 136964. [CrossRef]
7. Ma, X.Y.; Yang, W.; Kallio, H.; Yang, B.R. Health promoting properties and sensory characteristics of phytochemicals in berries and leaves of sea buckthorn (*Hippophaë rhamnoides*). *Crit. Rev. Food Sci. Nutr.* **2021**, *62*, 3798–3816. [CrossRef] [PubMed]
8. Wang, B.; Liu, Y.X.; Dong, M.; Zhang, Y.Y.; Huang, X.H.; Qin, L. Flavor enhancement during the drying of scallop (*Patinopecten yessoensis*) as revealed by integrated metabolomic and lipidomic analysis. *Food Chem.* **2024**, *432*, 137218. [CrossRef]
9. Joardder, M.U.H.; Karim, M.A. Drying kinetics and properties evolution of apple slices under convective and intermittent-MW drying. *Therm. Sci. Eng. Prog.* **2022**, *30*, 101279. [CrossRef]
10. Ju, H.Y.; Zou, Y.Z.; Xiao, H.W.; Zhang, W.P.; Yu, X.L.; Gao, Z.J. Effects of relative humidity on water diffusion and evaporation during hot air drying of carrot. *Trans. Chin. Soc. Agric. Eng.* **2023**, *39*, 232–240. Available online: https://kns.cnki.net/2023.39.01.232-240 (accessed on 23 February 2023).
11. Curcio, S.; Aversa, M.; Calabrò, V.; Iorio, G. Simulation of food drying: Fem analysis and experimental validation. *J. Food Eng.* **2008**, *87*, 541–553. [CrossRef]
12. Zhang, W.P.; Yang, X.H.; Mujumdar, A.S.; Ju, H.Y.; Xiao, H.W. The influence mechanism and control strategy of relative humidity on hot air drying of fruits and vegetables: A review. *Dry. Technol.* **2022**, *40*, 2217–2234. [CrossRef]

13. Geng, Z.; Li, M.; Zhu, L.; Zhang, X.; Zhu, H.; Yang, X.; Yu, X.; Zhang, Q.; Hu, H. Design and experiment of infrared combined hot-air dryer based on temperature and humidity control on sea buckthorn (*Hippophae rhamnoides* L.). *Foods* **2023**, *12*, 2299. [CrossRef] [PubMed]
14. Geng, Z.; Torki, M.; Beigi, M.; Kaveh, M.; Yang, X.H. Characteristics and multi-objective optimization of carrot dehydration in a hybrid infrared /hot air dryer. *LWT-Food Sci. Technol.* **2022**, *172*, 114229. [CrossRef]
15. Thao, B.T.T.; Vo, T.T.K.; Tran, T.Y.N.; Le, D.T.; Tran, T.T.; Bach, L.G.; Dao, T.P. Application of mathematical techniques to study the moisture loss kinetics and polyphenol degradation kinetics of mango (*Mangifera indica* L.) slices during heat pump drying by pilot equipment. *LWT-Food Sci. Technol.* **2023**, *176*, 114454. [CrossRef]
16. Guo, X.J.; Hao, Q.D.; Qiao, X.G.; Li, M.; Qiu, Z.C.; Zheng, Z.J.; Zhang, B. An evaluation of different pretreatment methods of hot-air drying of garlic: Drying characteristics, energy consumption and quality properties. *LWT-Food Sci. Technol.* **2023**, *180*, 114685. [CrossRef]
17. Chang, A.T.; Zheng, X.; Xiao, H.W.; Yao, X.D.; Liu, D.C.; Li, X.Y.; Li, Y.C. Short- and medium-wave infrared drying of Cantaloupe (*Cucumis melon* L.) slices: Drying kinetics and process parameter optimization. *Processes* **2022**, *10*, 114. [CrossRef]
18. Liu, Z.L.; Xie, L.; Zielinska, M.; Pan, Z.L.; Wang, J.; Deng, L.Z.; Wang, H.; Xiao, H.W. Pulsed vacuum drying enhances drying of blueberry by altering micro-ultrastructure and water status and distribution. *LWT-Food Sci. Technol.* **2021**, *142*, 111013. [CrossRef]
19. Deng, L.Z.; Yang, X.H.; Mujumdar, A.S.; Zhao, J.H.; Wang, D.; Zhang, Q.; Wang, J.; Gao, Z.J.; Xiao, H.W. Red pepper (*Capsicum annuum* L.) drying: Effects of different drying methods on drying kinetics, physicochemical properties, antioxidant capacity, and microstructure. *Dry. Technol.* **2018**, *36*, 893–907. [CrossRef]
20. Wang, H.; Liu, Z.L.; Vidyarthi, S.K.; Wang, Q.H.; Gao, L.; Li, B.R.; Wei, Q.; Liu, Y.H.; Xiao, H.W. Effect of different drying methods on drying kinetics, physicochemical properties, microstructure, and energy consumption of potato (*Solanum tuberosum* L.) cubes. *Dry. Technol.* **2021**, *39*, 418–431. [CrossRef]
21. Geng, Z.H.; Zhu, L.C.; Wang, J.; Yu, X.L.; Li, M.Q.; Yang, W.X.; Hu, B.; Zhang, Q.; Yang, X.H. Drying sea buckthorn berries (*Hippophae rhamnoides* L.): Effects of different drying methods on drying kinetics, physicochemical properties, and microstructure. *Front. Nutr.* **2023**, *10*, 1106009. [CrossRef]
22. Chu, Q.Q.; Li, L.L.; Duan, X.; Zhao, M.Y.; Wang, Z.K.; Wang, Z.; Ren, X.; Li, C.Y.; Ren, G.Y. Effect mechanism of different drying methods on the quality and browning for daylily. *LWT-Food Sci. Technol.* **2023**, *182*, 114862. [CrossRef]
23. Tan, S.D.; Xu, Y.; Zhu, L.C.; Geng, Z.H.; Zhang, Q.; Yang, X.H. Hot air drying of sea buckthorn (*Hippophae rhamnoides* L.) berries: Effects of different pretreatment methods on drying characteristics and quality attributes. *Foods* **2022**, *11*, 3675. [CrossRef]
24. Lee, S.Y.; Ferdinand, V.; Siow, L.F. Effect of drying methods on yield, physicochemical properties, and total polyphenol content of chamomile extract powder. *Front. Pharmacol.* **2022**, *13*, 1003209. [CrossRef] [PubMed]
25. Liu, Z.L.; Xie, L.; Zielinska, M.; Pan, Z.L.; Deng, L.Z.; Zhang, J.S.; Gao, L.; Wang, S.Y.; Zheng, Z.A.; Xiao, H.W. Improvement of drying efficiency and quality attributes of blueberries using innovative far-infrared radiation heating assisted pulsed vacuum drying (FIR-PVD). *Innov. Food Sci. Emerg. Technol.* **2022**, *77*, 102948. [CrossRef]
26. Liu, Z.L.; Zielinska, M.; Yang, X.H.; Yu, X.L.; Chen, C.; Wang, H.; Wang, J.; Pan, Z.L.; Xiao, H.W. Moisturizing strategy for enhanced convective drying of mushroom slices. *Renew. Energy* **2021**, *172*, 728–739. [CrossRef]
27. Deng, L.Z.; Xiong, C.H.; Pei, Y.P.; Zhu, Z.Q.; Zheng, X.; Zhang, Y.; Yang, X.H.; Liu, Z.L.; Xiao, H.W. Effects of various storage conditions on total phenolic, carotenoids, antioxidant capacity, and color of dried apricots. *Food Control.* **2022**, *136*, 108846. [CrossRef]
28. Wang, J.; Mujumdar, A.S.; Wang, H.; Fang, X.M.; Xiao, H.W.; Raghavan, V. Effect of drying method and cultivar on sensory attributes, textural profiles, and volatile characteristics of grape raisins. *Dry. Technol.* **2021**, *39*, 495–506. [CrossRef]
29. Xie, L.; Zheng, Z.A.; Mujumdar, A.S.; Fang, X.M.; Wang, J.; Zhang, Q.; Ma, Q.; Xiao, H.W.; Liu, Y.H.; Gao, Z.J. Pulsed vacuum drying (PVD) of wolfberry: Drying kinetics and quality attributes. *Dry. Technol.* **2018**, *36*, 1501–1514. [CrossRef]
30. Alfeo, V.; Planeta, D.; Velotto, S.; Palmeri, R.; Todaro, A. Cherry tomato drying: Sun versus convective oven. *Horticulturae* **2021**, *7*, 40. [CrossRef]
31. Jiang, D.L.; Xiao, H.W.; Zielinska, M.; Zhu, G.F.; Bai, T.Y.; Zheng, Z.A. Effect of pulsed vacuum drying of drying kinetics and quality of roots of *Panax notoginseng* (Burk) F. H. Chen (Araliaceae). *Dry. Technol.* **2022**, *39*, 2234–2251. [CrossRef]
32. Zhang, Y.; Zhu, G.F.; Li, X.Y.; Zhao, Y.; Lei, D.W.; Ding, G.Q.; Ambrose, K.; Liu, Y.H. Combined medium- and short-wave infrared and hot air impingement drying of sponge gourd (*Luffa cylindrical*) slices. *J. Food Eng.* **2020**, *284*, 110043. [CrossRef]
33. Hu, L.N.; Bi, J.F.; Jin, X.; Qiu, Y.; van der Sman, R.G.M. Study on the rehydration quality improvement of shiitake mushroom by combined drying methods. *Foods* **2021**, *10*, 769. [CrossRef] [PubMed]
34. Geng, Z.H.; Wang, J.; Zhu, L.C.; Yu, X.L.; Zhang, Q.; Li, M.Q.; Hu, B.; Yang, X.H. Metabolomics provide a novel interpretation of the changes in flavonoids during sea buckthorn (*Hippophae rhamnoides* L.) drying. *Food Chem.* **2023**, *413*, 135598. [CrossRef] [PubMed]